

Annual Progress Report: Validation of AMSR-E Snow Products (NAG5-11107)

March 30, 2004

From: Richard L. Armstrong
CIRES/NSIDC, University of Colorado, Boulder, CO 80309

To: David O'C. Starr, Head, Mesoscale Atmospheric Processes Branch, Code 912, NASA
GSFC, Greenbelt, MD 20771

I. Background and Legacy Data

The extent of the seasonal snow cover, which may include as much as 50 percent of the Northern Hemisphere land surface, is an extremely important parameter in global climate and hydrologic systems due to significant effects on energy and moisture budgets. Realistic simulation of snow cover in climate models is essential for correct representation of the surface energy balance, as well as for understanding winter water storage and predicting year-round runoff. Passive microwave signatures of seasonal snow cover are clearly characterized by a strong dielectric contrast between snow-covered and snow-free ground, by decreasing emissivity with increasing microwave frequency (negative spectral gradient) and by decreasing emissivity with increasing snow mass. Because of this clear capability, a microwave snow cover algorithm is included in the suite of algorithms supported by the AMSR-E Science Team.

The AMSR-E snow products will contribute to one of the longest time series of any environmental product derived from satellite remote sensing. The National Snow and Ice Data Center (NSIDC) has produced a 25-year, consistently processed, time series of gridded satellite passive microwave data in a common format called the Equal-Area Scalable Earth Grid (EASE-Grid). This data set was developed using SMMR (Scanning Multichannel Microwave Radiometer) data for the period 1978 to 1987 and SSM/I (Special Sensor Microwave Imager) data for 1987 to 2003 and has been used to derive a series of snow and ice products. Figure 1 shows the time series for Northern Hemisphere snow cover and includes data from the NOAA visible satellites for comparison.

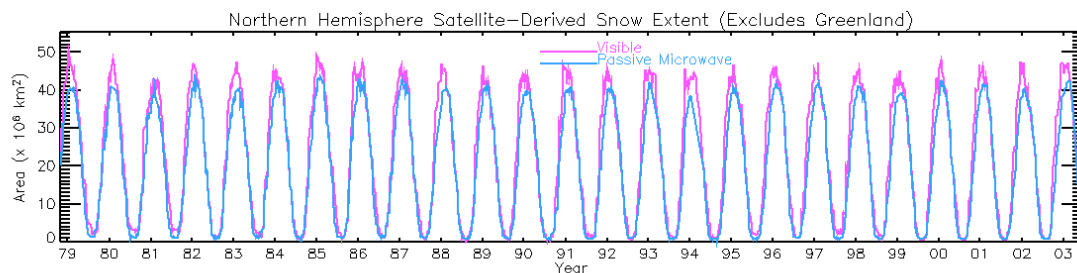


Figure.1. Northern Hemisphere snow-covered area ($\times 10^6$ km²) derived from visible (NOAA) and passive microwave (SMMR and SSM/I) satellite data, 1978-2003.

II. Progress and Accomplishments

A. Interaction with the EOS AMSR-E Science Team

The snow algorithm team responded to a number of our concerns raised in last year's report. For example, they satisfactorily addressed the issue regarding the data range of values. We continue to collaborate on various masks being used. We have provided the algorithm team with a new version of the land-ocean-permanent ice mask, derived from the International Geosphere-Biosphere Programme (IGBP) Global Land Cover Classification (GLCC) data. At the request of

Richard Kelly, we are evaluating the use of a new MODIS land mask to replace the GLCC in a future version of the processing. We have provided the historical monthly average SWE derived from SSM/I (1987-2003) to the algorithm team for use in time series analysis. We recommend that the current static snow extent climatology be replaced by monthly climatologies derived from the NOAA weekly snow charts.

We evaluated and commented on the standard snow algorithm examples released in February 2004. The example data were adversely affected by an orbital maneuver, and we suggested that such data might be eliminated by a change to the algorithm that would check orbital metadata. The algorithm team is exploring this possibility for a future release. We have also identified some discrepancies in the snow product documentation, and brought the corrections to the attention of the NSIDC documentation team.

B. Summary of data flow following the May 4, 2002 launch.

During 2003, data using the RSS preliminary calibration, known as “X1” data, were replaced by data using the final calibration, referred to as the “B01” version of the data. During the period covered by this report, we began to evaluate B01 data in place of X1 data whenever it was available. AMSR-E B01 data are currently available from launch to near real-time.

C. Comparison of AMSR-E with other satellite products

1. Brightness temperatures - SSM/I

As a baseline accuracy check, we have compared AMSR-E brightness temperatures for a snow covered surface with SSM/I brightness temperatures at Dome C in Antarctica (74.5S, 123.0E) (Figure 2). A site such as Dome C was selected because it represents a target with microwave emissivity that is reasonably consistent across an area comparable to a passive microwave satellite sensor footprint. Therefore, the annual time series is primarily a response to fluctuations in physical temperature.

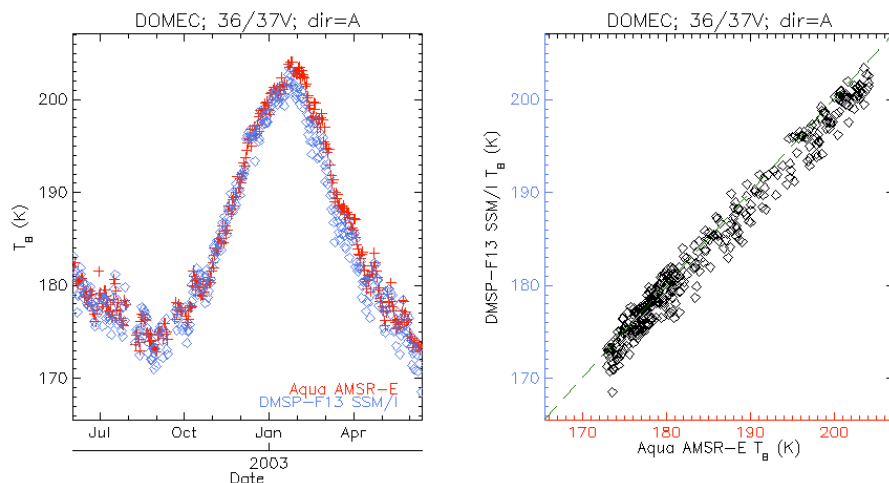


Figure 2. Comparison of AMSR-E and SSM/I brightness temperatures at Dome C, Antarctica, (2002-2003).

In this example we compare vertically polarized 36/37 GHz data. The increased variability in both signals during the winter (July-September) is caused by the cycling of katabatic winds that remove the near surface temperature inversion resulting in higher physical temperatures. The slight positive bias shown by AMSR-E 36 GHz is possibly due to the lower frequency. Overpass times in this example are coincident.

2. Snow Extent – Comparison of passive microwave and optical data.

a. Background

Because products from the standard NASA AMSR-E Science Team snow algorithm (Kelly et al. 2003) only recently became available (March 1, 2004), and more importantly because there were some minor problems with the initial processing of these data, we have chosen not to directly validate those products at this time. In the near future, all of our validation studies will focus on the standard Science Team products. In the meantime, we have made use of the B01 version AMSR-E Level 2A Brightness Temperature data as it has been made available to the validation team. We have derived SWE from these AMSR-E data using a modified version of the original Chang SMMR algorithm (Armstrong and Brodzik, 2001) and have implemented the forest correction by Chang et al. (1996) as well as precipitation filters optimized for SSM/I by Grody and Basist (1996). Our general algorithmic approach approximates that taken by the AMSR-E algorithm team and we expect results of future comparisons with the standard snow product to be similar to the results presented here. We look forward to examining the full time series of the standard snow product using the methods presented here.

Previous studies have shown that, compared to optical data, current passive microwave snow algorithms tend to undermeasure snow extent over large areas in early fall, and at the edges of the seasonal snow pack, where snow is typically shallow and/or intermittent (Armstrong and Brodzik, 2001; 2002). This underestimate of snow extent results from at least two factors; 1) shallow snow cover (less than about 5.0 cm) often possibly combined with wet snow, does not provide a scattering signal of sufficient strength to be detected by the algorithms and 2) even when snow exists at greater depths across the microwave sensor field of view but is intermittent in extent, the scattering signature integrated over this mixed pixel is not adequate to trigger current microwave algorithms. As the snow cover continues to build during the winter months and on into the melt season, agreement between the two data types continually improves. This occurs because as the snow becomes deeper and more continuous in extent and the layered structure becomes more complex, the negative spectral gradient driving the passive microwave algorithm is enhanced. The increased accuracy during spring melt is fortunate as this is the most important period of the snow cover season in terms of snow hydrology, thus allowing confident application of these snow water equivalent data to hydrologic forecasting and modeling.

b. Blending microwave and optical data

Because the current AMSR-E snow algorithms do not differ fundamentally from the earlier SSM/I algorithms, this pattern of seasonal dependency of snow extent underestimation by passive microwave persists. This can be seen in Figure 3, which combines AMSR-E-derived snow water equivalent with MODIS snow cover for examples during fall and spring of 2003. Snow cover for two 8-day periods derived from SSM/I and from AMSR-E shows good agreement, with some differences in SWE. (The algorithms are not yet intercalibrated.)

c. Quantitative comparison with MODIS snow extent.

We have developed a method to quantify the relationship between passive microwave snow retrievals and MODIS snow extent. Figure 4 shows a histogram that determines the threshold at which a microwave algorithm begins to detect snow cover. In this example, for the Northern Hemisphere on March 11, 2003, each EASE-Grid pixel (625 km^2) is assigned a percent MODIS

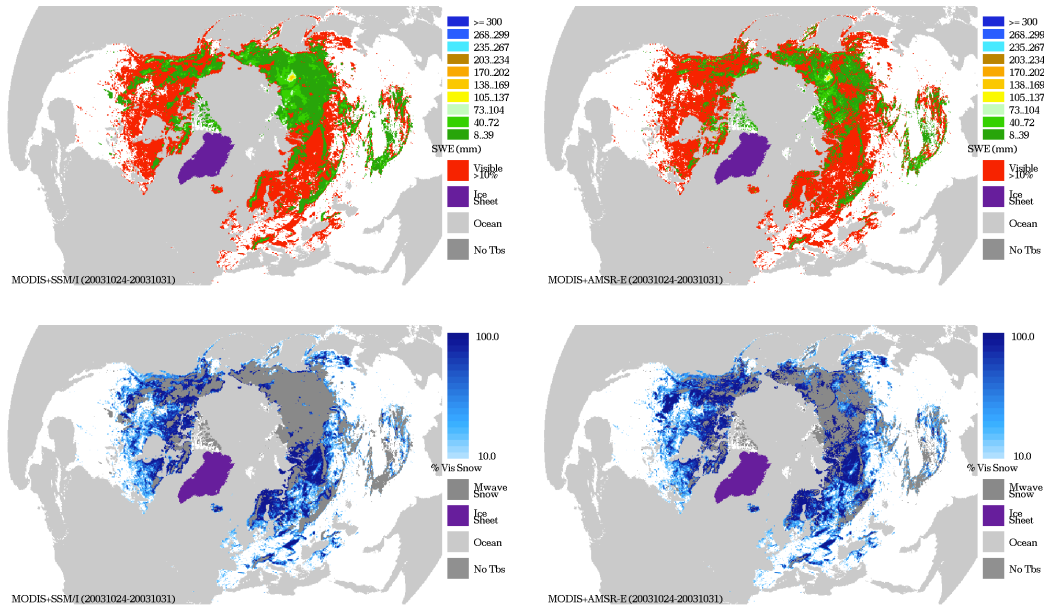


Figure 3a. Blended snow prototypes, SWE (from SSM/I (left side) and AMSR-E (right side)) with snow cover from MODIS, Fall, 2003. Top panels in each set of four represent SWE (mm), with additional area indicated as snow by MODIS in red. Lower panels represent passive microwave snow extent in grey, with percent area of additional pixels that MODIS classifies as snow in blues.

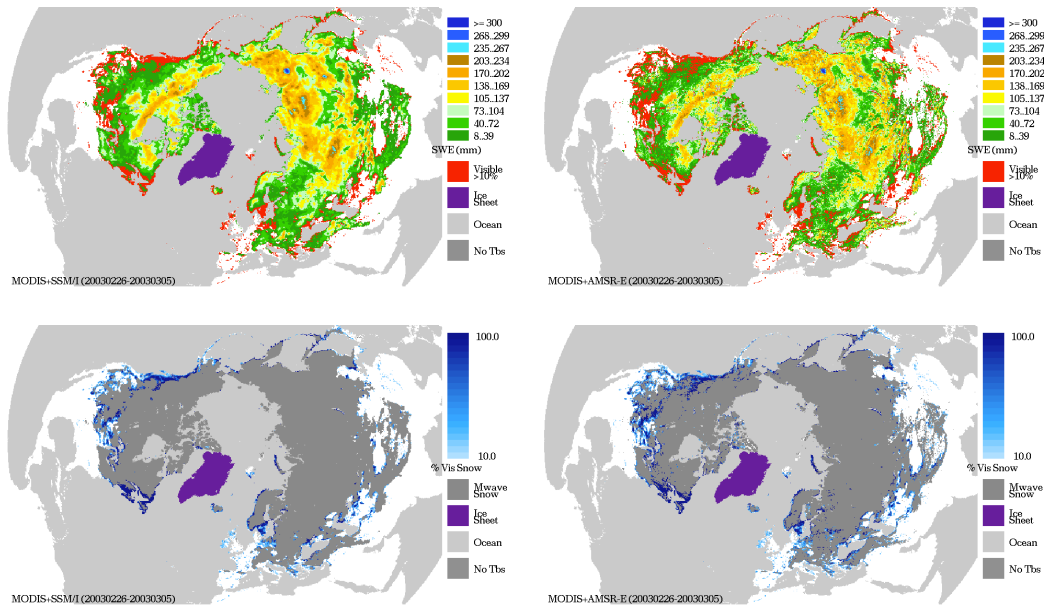


Figure 3b. Same as 3a, Spring, 2003.

snow covered area by calculating the average of the 0.05 deg. Climate Modelers Grid (CMG) MODIS snow product. A second histogram is generated by counting the number of pixels in each MODIS percent bin where the passive microwave algorithm detected a SWE of greater than zero. The ratio of these two histograms is used to generate the monthly data shown in Figure 5, which presents this threshold throughout the winter season.

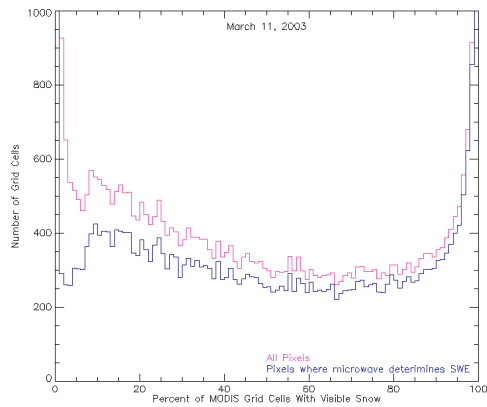


Figure 4. Histogram to determine threshold at which microwave begins to detect snow.

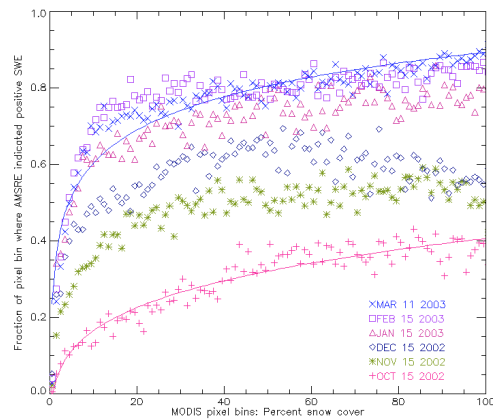


Figure 5. Microwave SWE Threshold representing the fraction of all pixels examined positive SWE as a function of MODIS percent snow cover.

Figure 5 shows how as percent snow cover in a grid cell increases, the more likely the passive microwave algorithm will detect the presence of snow cover. As the winter season progresses, less snow cover is needed to trigger a response from the microwave algorithm. For example, in October, 50% snow cover from MODIS causes a microwave response of greater than zero in only about 30% of the pixels while even 100% snow cover only triggers a response in about 40% of the cases. In contrast, later in the season, during February and March, 50% MODIS snow cover corresponds to about 75 to 85%. This method will be used in our future evaluations of the accuracy of the standard AMSR-E snow products.

d. Examples of enhanced spatial resolution provided by AMSR-E data.

Comparison of snow cover derived from MODIS, SSM/I and AMSR-E over the Tibet Plateau provides a clear example of the higher spatial resolution of AMSR-E yielding more accurate snow extent maps (Figure 6). The Tibet Plateau typically receives only small snowfall amounts, often

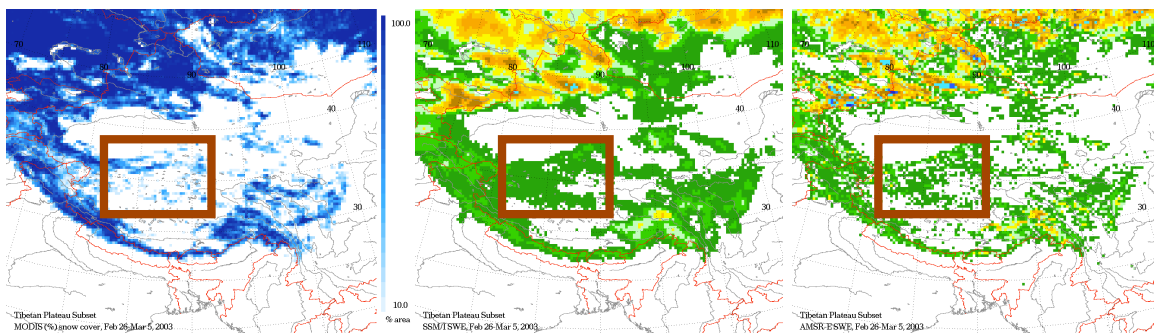


Figure 6. Tibetan Snow Cover, February 26 - March 5, 2003, left to right: percent area with MODIS snow, SWE derived from SSM/I and SWE derived from AMSR-E. Red box outlines area of patchy visible snow (MODIS) that is smoothed by SSM/I but better resolved by AMSR-E's improved spatial resolution.

accompanied by strong winds. This results in a pattern of spatially intermittent, i.e. patchy, shallow snow cover, which is apparent in the MODIS image. The coarse resolution SSM/I data are not capable of resolving this pattern of intermittent snow, in essence spatially smoothing the pattern and appearing as continuous thin snow cover. The smaller footprint of the AMSR-E,

however, provides a much improved capability to identify these smaller individual areas of patchy snow cover. This example demonstrates the potential value of AMSR-E snow data over smaller hydrologic catchment basins with intermittent snow cover. In future investigations we will explore the potential to enhance the spatial resolution of the AMSR-E brightness temperatures using advanced re-sampling techniques.

3. Snow Water Equivalent (SWE) and snow depth comparisons with SSM/I and other validation data sets.

a. Comparison of Mean monthly SWE from AMSR-E and SSM/I

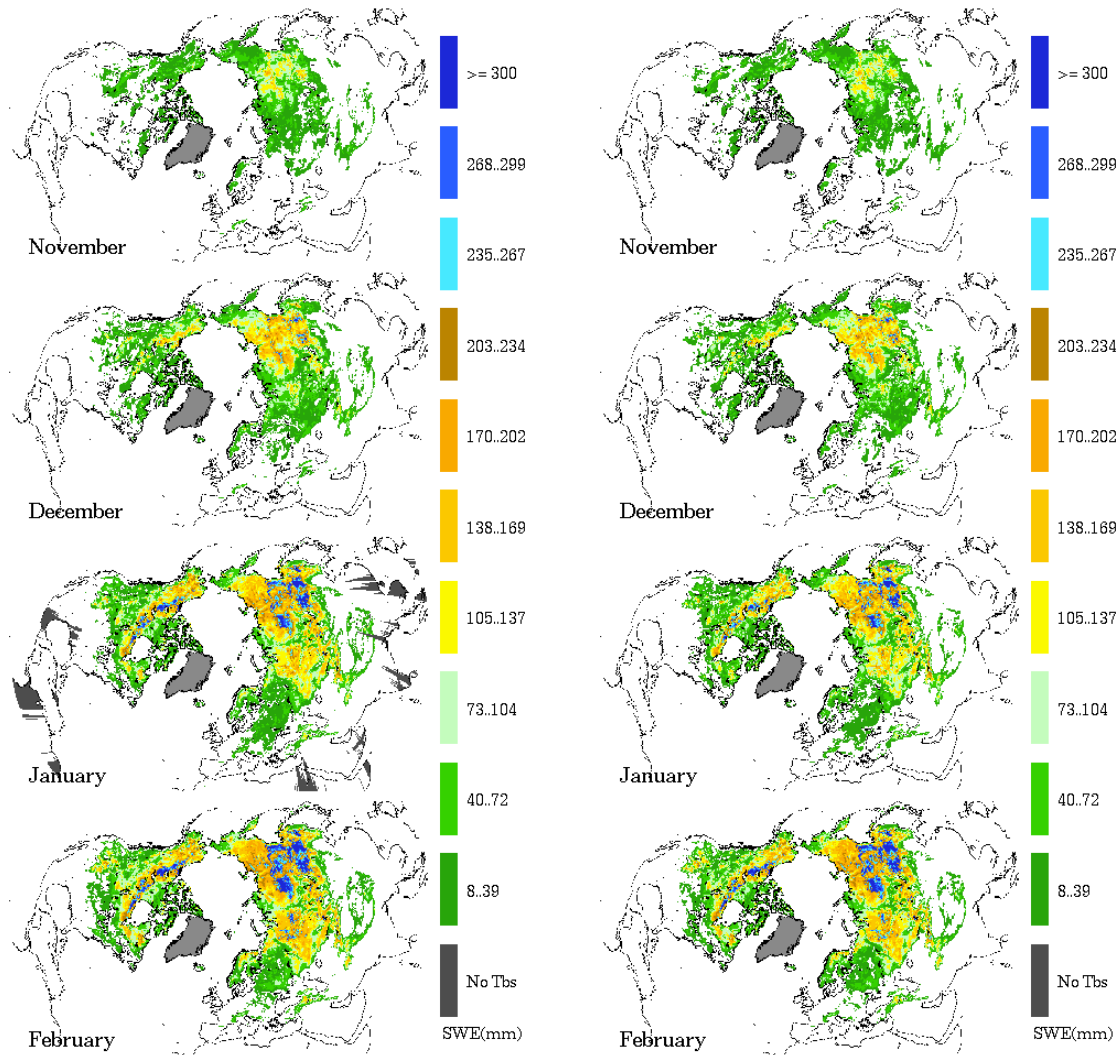


Figure 7. Northern Hemisphere monthly average snow water equivalent derived from SSM/I (left) and AMSR-E (right), November 2003 – February 2004.

Figure 7 compares monthly average SWE derived from AMSR-E and SSM/I brightness temperatures for November 2003 to February 2004. Both the absolute values and the spatial patterns of the two data sets are similar. In order to eventually merge the AMSR-E snow products with the SSM/I data to produce a single climate data record, it will be necessary to adjust the AMSR-E brightness temperatures to match the SSM/I. The results of this preliminary comparison indicate that the intercalibration adjustments will be small.

b. NASA Cold Lands Processes Experiment

Our validation study benefits from direct participation in the NASA Cold Land Processes Experiment (CLPX) which took place during mid-February and late March 2003 in northwestern Colorado. The CLPX was described in detail in our 2003 report and current information can be found at <http://www.nohrsc.nws.gov/~cline/clp.html>. Figure 8 shows the AMSR-E-derived snow water equivalent (SWE) for the Large Regional Study Area including the three Meso-cell Study Areas (MSAs) for February 23, 2003. The comprehensive analysis of the CLPX data and the use of these data to validate the AMSR-E snow algorithms is currently underway and results will appear in subsequent reports and presentations.

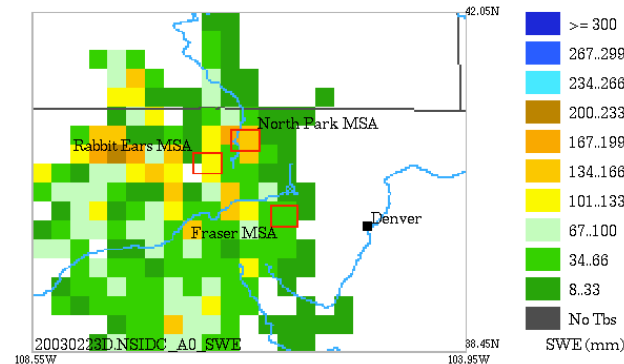


Figure 8. Snow water equivalent derived from AMSR-E for CLPX LRSA, (—degree lat-lon grid), February 23, 2003.

In conjunction with the CLPX we operated the University of Tokyo Ground Based Microwave Radiometer (GBMR-7), an AMSR-E simulator for the higher frequency channels (18.7, 23.8, 36.5 and 89.0 GHz) during 2003 at the Fraser Experimental Forest. In developing the snow algorithm it has been found that the snow grain size distribution is one of the most critical parameters. With a priori grain size profiles built into the algorithm, snow retrieval accuracy can be improved. Field experiments associated with the operation of the GBMR-7 measured snow grain size distribution, variation with time and influence on microwave emission. Only limited preliminary results from these 2003 data are available (Figure 9) while a comprehensive analysis is currently underway. Note how the higher resolution AMSR-E data agree more closely with the ground-based measurements (snow pits) and the GBMR-7 data than do the SSM/I data.

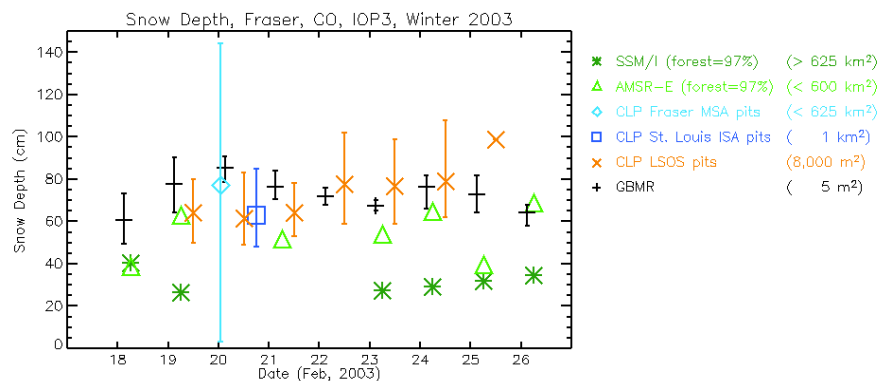


Figure 9. Snow depth at CLPX Fraser MSA, various measurement techniques and spatial resolutions, IOP3, March, 2003.

III. Conclusions

As a baseline accuracy and stability check of brightness temperatures over a snow surface, we have compared AMSR-E with SSM/I at Dome C in Antarctica. Although similar comparisons are being undertaken by other members of the EOS AMSR-E science team over other land surface types, it is important to include brightness temperature comparisons over a surface with the spectral signature of snow. This comparison shows a very close relationship between the two data sets.

Other examples in this report compare AMSR-E-derived snow data with other snow extent and water equivalent data. In these examples we primarily use the NSIDC6 algorithm, which is fundamentally similar to the Science Team algorithm. The results of these tests clearly demonstrate basic accuracy, integrity and consistency of the AMSR-E brightness temperatures when applied to snow cover retrievals. All future validation work will focus on the standard Science Team snow products using the various methodologies and validation data sets described in this report.

IV. Future Work – Plans for Year 3

Specific validation studies are currently, or soon will be, underway using the following validation data sets.

A. Local or grid scale validation

1. All appropriate data from CLPX 2003 as described above.
2. National Weather Service (NWS) Cooperative Network (COOP) snow depth and snow water equivalent data, 2002-2004.
3. Snow depth data for 2002-2003 for the Tibet plateau to be provided by the Cold and Arid Regions Environmental and Engineering Institute (CAREERI) Lanzhou, China, during April 2004.

B. Large river basin scale validation

Larger river basin scale validation is being undertaken through participation in Arctic-RIMS, an ongoing NASA and NSF funded program that involves the integrated near-real time monitoring and analysis of the major components of the pan-Arctic hydrologic cycle. Output from the AMSR-E snow algorithm will be compared with river discharge data as well as with modeled values of distributed winter precipitation.

C. Regional to hemispheric scale validation

We will continue to evaluate the AMSR-E snow algorithms by comparison with MODIS and NOAA IMS snow extent maps and SSM/I-derived SWE data.

V. Data Management and Archival

All pertinent data resulting from this validation study will be archived at the National Snow and Ice Data Center (NSIDC), University of Colorado, Boulder. Selected data sets will be available to the wider scientific community through NSIDC's User Services Office (nsidc@nsidc.org).

VI. References:

- Armstrong, R.L. and M.J. Brodzik. 2002. Hemispheric-scale comparison and evaluation of passive microwave snow algorithms. *Annals of Glaciology* 34:38-44.
- Armstrong, R.L. and M.J. Brodzik, 2001. Recent Northern Hemisphere snow extent: a comparison of data derived from visible and microwave sensors. *Geophysical Research Letters* 28(19):3673-3676.
- Chang, A.T.C., J.L. Foster, and D.K. Hall. 1996. Effects of forest on the snow parameters derived from microwave measurements during the BOREAS winter field campaign. *Hydrological Processes* 10:1565-1574.
- Cline, D. 2001. NASA Cold Land Processes Field Experiment Plan 2002-2004. Cold Land Processes Working Group, NASA Earth Science Enterprise, Land Surface Hydrology Program, unpublished draft report.
- Grody, Norman C. and Alan N. Basist. 1996. Global Identification of Snowcover Using SSM/I Measurements, *IEEE Transactions on Geoscience and Remote Sensing* 34(1):237-249.
- Kelly, R.E., A.T.C. Chang, L. Tsang, and J.L. Foster. 2003. A prototype AMSR-E global snow area and snow depth algorithm. *IEEE Transactions on Geoscience and Remote Sensing* 41(2): 230-242.